

1 **A GENERALISED RANDOM ENCOUNTER MODEL FOR ESTIMATING**
2 **ANIMAL DENSITY WITH REMOTE SENSOR DATA**

3 **Running title: A generalised random encounter model for animals.**

4 **Word count:**

5 **Authors:**

6 Tim C.D. Lucas^{1,2,3}, Elizabeth A. Moorcroft^{1,4,5}, Robin Freeman⁵, Marcus J. Rowcliffe⁵,
7 Kate E. Jones^{2,5}

8 **Addresses:**

9 1 CoMPLEX, University College London, Physics Building, Gower Street, Lon-
10 don, WC1E 6BT, UK

11 2 Centre for Biodiversity and Environment Research, Department of Genetics,
12 Evolution and Environment, University College London, Gower Street, London,
13 WC1E 6BT, UK

14 3 Department of Statistical Science, University College London, Gower Street,
15 London, WC1E 6BT, UK

16 4 Department of Computer Science, University College London, Gower Street,
17 London, WC1E 6BT, UK

18 5 Institute of Zoology, Zoological Society of London, Regents Park, London, NW1
19 4RY, UK

20 **Corresponding authors:**

21 Kate E. Jones,
22 Centre for Biodiversity and Environment Research,
23 Department of Genetics, Evolution and Environment,
24 University College London,
25 Gower Street,
26 London,
27 WC1E 6BT,
28 UK

29 kate.e.jones@ucl.ac.uk

30

31 Marcus J. Rowcliffe,

32 Institute of Zoology,

33 Zoological Society of London,

34 Regents Park,

35 London,

36 NW1 4RY,

37 UK

38 marcus.rowcliffe@ioz.ac.uk

ABSTRACT

39
40 **1:** Wildlife monitoring technology has advanced rapidly and the use of remote
41 sensors such as camera traps, and acoustic detectors is becoming common in both
42 the terrestrial and marine environments. Current methods to estimate abundance
43 or density require individual recognition of animals or knowing the distance of
44 the animal from the sensor, which is often difficult. A method without these re-
45 quirements, the random encounter model (REM), has been successfully applied to
46 estimate animal densities from count data generated from camera traps. However,
47 count data from acoustic detectors do not fit the assumptions of the REM due to
48 the directionality of animal signals.

49 **2:** We developed a generalised REM (gREM), to estimate absolute animal density
50 from count data from both camera traps and acoustic detectors. We derived the
51 gREM for different combinations of sensor detection widths and animal signal
52 widths (a measure of directionality). We tested the accuracy and precision of this
53 model using simulations of different combinations of sensor detection widths and
54 animal signal widths, number of captures, and models of animal movement.

55 **3:** We find that the gREM produces accurate estimates of absolute animal density
56 for all combinations of sensor detection widths and animal signal widths. How-
57 ever, larger sensor detection and animal signal widths were found to be more pre-
58 cise. While the model is accurate for all capture efforts tested, the precision of the
59 estimate increases with the number of captures. We found no effect of different
60 animal movement models tested on the accuracy and precision of the gREM.

61 **4:** We conclude that the gREM provides an effective method to estimate absolute
62 animal densities from remote sensor count data over a range of sensor and animal
63 signal widths. The gREM is applicable for count data obtained in both marine and
64 terrestrial environments, visually or acoustically (e.g., big cats, sharks, birds, bats
65 and cetaceans). As sensors such as camera traps and acoustic detectors become
66 more ubiquitous, the gREM will be increasingly useful for monitoring unmarked
67 animal populations across broad spatial, temporal and taxonomic scales.

Keywords. acoustic detection, camera traps, marine, population monitoring, simulations, terrestrial

INTRODUCTION

Animal population density is one of the fundamental measures needed in ecology and conservation. The density of a population has important implications for a range of issues such as sensitivity to stochastic fluctuations (Richter-Dyn & Goel, 1972; Wright & Hubbell, 1983) and risk of extinction (Purvis *et al.*, 2000). Monitoring animal population changes in response to anthropogenic pressure is becoming increasingly important as humans modify habitats and change climates as never before (Everatt *et al.*, 2014). Sensor technology, such as camera traps (Rowcliffe & Carbone, 2008; Karanth, 1995) and acoustic detectors (O’Farrell & Gannon, 1999; Clark, 1995; Acevedo & Villanueva-Rivera, 2006) are becoming increasingly used to monitor changes in animal populations (Rowcliffe & Carbone, 2008; Kessel *et al.*, 2014), as they are efficient, relatively cheap and non-invasive (Cutler & Swann, 1999), allowing for surveys over large areas and long periods. However, the problem of converting sampled count data to estimates of density remains as efforts must be made to account for detectability of the animals (Anderson, 2001).

Methods do already exist for estimating animal density but these methods often require additional information that may not be available. For example, capture-mark-recapture methods (Karanth, 1995; Trolle & Kéry, 2003; Soisalo & Cavalcanti, 2006; Trolle *et al.*, 2007; ?) require recognition of individuals, distance methods (Harris *et al.*, 2013) require an estimation of how far away individuals are from the sensor (Barlow & Taylor, 2005; Marques *et al.*, 2011). The development of the random encounter model (REM) (a modification of a gas model) enabled animal densities to be estimated from unmarked individuals of a known speed, and sensor detection parameters (Rowcliffe *et al.*, 2008). The REM method has been successfully applied to estimate animal densities from camera trap surveys (Manzo *et al.*, 2012; Zero *et al.*, 2013). However, extending the REM method to other types of sensors (for example acoustic detectors) is more problematic, because the original derivation assumes a relatively narrow sensor width (up to $\pi/2$ radians) and that the animal is equally detectable irrespective of its heading (Rowcliffe *et al.*, 2008).

99 Whilst these restrictions are not problematic for most camera trap makes (e.g.
100 Reconyx, Cuddeback), the REM could not be used to estimate densities from cam-
101 era traps with a wider sensor width (e.g. canopy monitoring with fish eye lens
102 (Brusa & Bunker, 2014)). Additionally, the REM method would not be useful in
103 estimating densities from acoustic survey data as the acoustic detector angles are
104 often wider than $\pi/2$ radians. Acoustic detectors are designed for a range of di-
105 verse tasks and environments (Kessel *et al.*, 2014), which will naturally lead to a
106 wide range of sensor detection widths and detection distances. In addition to this,
107 calls emitted by many animals are directional (Blumstein *et al.*, 2011) breaking the
108 assumption of the REM method.

109 There has been a sharp rise in interest around passive acoustic detectors in re-
110 cent years, with a 10 fold increase in publications in the decade between 2000 and
111 2010 (Kessel *et al.*, 2014). Acoustic monitoring is being developed to study many
112 aspects of ecology, including the interactions of animals and their environments
113 (Blumstein *et al.*, 2011; Rogers *et al.*, 2013), the presence and relative abundances of
114 species (Marcoux *et al.*, 2011), and biodiversity of an area (Depraetere *et al.*, 2012).

115 Acoustic data suffers from many of the problems associated with data from
116 camera trap surveys in that individuals are often unmarked so capture-mark-
117 recapture methods cannot be used to estimate densities. In some cases the dis-
118 tance between the animal and the sensor is known, for example when an array of
119 sensors and the position of the animal is estimated by triangulation (Lewis *et al.*,
120 2007). In these situations distance-sampling methods can be applied, a method
121 typically used for marine mammals (Rogers *et al.*, 2013). However, in many cases
122 distance estimation is not possible, for example when single sensors are deployed,
123 a situation typical in the majority of terrestrial acoustic surveys (Elphick, 2008;
124 Buckland *et al.*, 2008). In these cases, only relative measures of local abundance can
125 be calculated, and not absolute densities. This means that comparison of popula-
126 tions between species and sites is problematic without assuming equal detectabil-
127 ity (Schmidt, 2003; ?; Walters *et al.*, 2013). Equal detectability is unlikely because of
128 differences in environmental conditions, sensor type, habitat, species biology.

129 In this study we create a generalised REM (gREM), as an extension to the cam-
130 era trap model of (Rowcliffe *et al.*, 2008), to estimate absolute density from count

131 data from acoustic detectors, or camera traps, where the sensor width can vary
 132 from 0 to 2π radians, and the signal given from the animal can be directional. We
 133 assessed the accuracy and precision of the gREM within a simulated environment,
 134 by varying the sensor detection widths, animal signal widths, number of captures
 135 and models of animal movement. We use the simulation results to recommend
 136 best survey practice for estimating animal densities from remote sensors.

137 METHODS

138 **Analytical Model.** The REM presented by Rowcliffe *et al.* (2008) adapts the gas
 139 model to model count data from camera trap surveys. The REM is derived assum-
 140 ing a stationary sensor with a detection width less than $\pi/2$ radians. However, in
 141 order to apply this approach more generally, and in particular to acoustic detec-
 142 tors, we need both to relax the constraint on sensor detection width, and allow
 143 for animals with directional signals. Consequently, we derive the gREM for any
 144 detection width, θ , between 0 and 2π with a detection distance r giving a circular
 145 sector within which animals can be captured (the detection zone)(Figure 1). Ad-
 146 ditionally, we model the animal as having an associated signal width α between
 147 0 and 2π (Figure 1, see Appendix S1 for a list of symbols). We start deriving the
 148 gREM with the simplest situation, the gas model where $\theta = 2\pi$ and $\alpha = 2\pi$.

149 *Gas Model.* Following Yapp (1956), we derive the gas model where sensors can
 150 capture animals in any direction and animal's signal is detectable from any direction($\theta =$
 151 2π and $\alpha = 2\pi$). We assume that animals are in a homogeneous environment, and
 152 move in straight lines of random direction with velocity v . We allow that our sta-
 153 tionary sensor can capture animals at a detection distance r and that if an animal
 154 moves within this detection zone they are captured with a probability of one, while
 155 animals outside the zone are never captured.

156 In order to derive animal density, we need to consider relative velocity from
 157 the reference frame of the animals. Conceptually, this requires us to imagine that
 158 all animals are stationary and randomly distributed in space, while the sensor
 159 moves with velocity v . If we calculate the area covered by the sensor during the
 160 survey period we can estimate the number of animals the sensor should capture.
 161 As a circle moving across a plane, the area covered by the sensor per unit time is

162 $2rv$. The number of expected captures, z , for a survey period of t , with an animal
163 density of D is $z = 2rvtD$. To estimate the density, we rearrange to get $D = z/2rvt$.

164 *gREM derivations for different detection and signal widths.* Different combinations of
165 θ and α would be expected to occur (e.g., sensors have different detection widths
166 and animals have different signal widths). For different combinations θ and α , the
167 area covered per unit time is no longer given by $2rv$. Instead of the size of the
168 sensor detection zone having a diameter of $2r$, the size changes with the approach
169 angle between the sensor and the animal. For any given signal width and detec-
170 tor width and depending on the angle that the animal approaches the sensor, the
171 width of the area within which an animal can be detected is called the profile, p .
172 The size of the profile (averaged across all approach angles) is defined as the aver-
173 age profile \bar{p} . However, different combinations of θ and α need different equations
174 to calculate \bar{p} .

175 We have identified the parameter space for the combinations of θ and α for
176 which the derivation of the equations are the same (defined as sub-models in the
177 gREM) (Figure 2). For example, the gas model becomes the simplest gREM sub-
178 model (upper right in Figure 2) and the REM from Rowcliffe *et al.* (2008) is another
179 gREM sub-model where $\theta < \pi/2$ and $\alpha = 2\pi$. We derive one gREM sub-model SE2
180 as an example below, where $2\pi - \alpha/2 < \theta < 2\pi$, $0 < \alpha < \pi$ (see Appendix S2 for
181 other gREM sub-models).

182 *Example derivation of SE2.* In order to calculate \bar{p} , we have to integrate over the
183 focal angle, x_1 (Figure ??). This is the angle taken from the centre line of the sensor.
184 Other focal angles are possible (x_2, x_3, x_4) and are used in other gREM sub-models
185 (see Appendix S2). As the size of the profile depends on the approach angle, we
186 present the derivation across all approach angles. When the sensor is directly
187 approaching the animal $x_1 = \pi/2$.

188 Starting from $x_1 = \pi/2$ until $\theta/2 + \pi/2 - \alpha/2$, the size of the profile is $2r \sin \alpha/2$
189 (Figure ??a). During this first interval, the size of α limits the width of the profile.
190 When the animal reaches $x_1 = \theta/2 + \pi/2 - \alpha/2$ (Figure ??b), the size of the profile is
191 $r \sin(\alpha/2) + r \cos(x_1 - \theta/2)$ and the size of θ and α both limit the width of the profile
192 (Figure ??c). Finally, at $x_1 = 5\pi/2 - \theta/2 - \alpha/2$ until $x_1 = 3\pi/2$, the width of the

193 profile is again $2r \sin \alpha/2$ (Figure ??d) and the size of α again limits the width of
194 the profile.

195 The profile width p for π radians of rotation (from directly towards the sensor
196 to directly behind the sensor) is completely characterised by the three intervals
197 (Figure ??b–d). Average profile width \bar{p} is calculated by integrating these profiles
198 over their appropriate intervals of x_1 and dividing by π which gives

$$\bar{p} = \frac{1}{\pi} \left(\int_{\frac{\pi}{2}}^{\frac{\pi}{2} + \frac{\theta}{2} - \frac{\alpha}{2}} 2r \sin \frac{\alpha}{2} dx_1 + \int_{\frac{\pi}{2} + \frac{\theta}{2} - \frac{\alpha}{2}}^{\frac{5\pi}{2} - \frac{\theta}{2} - \frac{\alpha}{2}} r \sin \frac{\alpha}{2} + r \cos \left(x_1 - \frac{\theta}{2} \right) dx_1 + \int_{\frac{5\pi}{2} - \frac{\theta}{2} - \frac{\alpha}{2}}^{\frac{3\pi}{2}} 2r \sin \frac{\alpha}{2} dx_1 \right) \quad \text{eqn 1}$$

$$= \frac{r}{\pi} \left(\theta \sin \frac{\alpha}{2} - \cos \frac{\alpha}{2} + \cos \left(\frac{\alpha}{2} + \theta \right) \right) \quad \text{eqn 2}$$

199 We then use this expression to calculate density

$$200 \quad D = z/vt\bar{p}. \quad \text{eqn 3}$$

201 Rather than having one equation that describes \bar{p} globally, the gREM must be
202 split into submodels due to discontinuous changes in p as α and β change. These
203 discontinuities can occur for a number of reasons such as a profile switching be-
204 tween being limited by α and θ , the difference between very small profiles and
205 profiles of size zero and the fact that the width of a sector stops increasing once
206 the central angle reaches π radians (i.e., a semi circle is just as wide as a full circle.)

207 As a visual example, if α is small, there is an interval between Figure ??c and ??d
208 where the ‘blind spot’ would prevent animals being detected at all giving $p = 0$.
209 This would require an extra integral in our equation as simply putting our small
210 value of α into eqn 1 would not give us this integral of $p = 0$.

211 gREM submodel specifications were done by hand, and the integration was
212 done using SymPy (SymPy Development Team, 2014) in Python (Appendix S3).
213 The gREM submodels were checked by confirming that: (1) submodels adjacent
214 in parameter space were equal at the boundary between them; (2) submodels that
215 border $\alpha = 0$ had $p = 0$ when $\alpha = 0$; (3) average profile widths \bar{p} were between 0
216 and $2r$ and; (4) each integral, divided by the range of angles that it was integrated

over, was between 0 and $2r$. The scripts for these tests are included in Appendix S3 and the R (R Development Core Team, 2010) implementation of the gREM is given in Appendix S4.

Simulation Model. We tested the accuracy and precision of the gREM by developing a spatially explicit simulation of the interaction of sensors and animals using different combinations of sensor detection widths, animal signal widths, number of captures, and models of animal movement. 100 simulations were run where each consisted of a 7.5 km by 7.5 km square with periodic boundaries. A stationary sensor of radius r was set up in the exact centre of each simulation, covering 7 sensor detection widths θ between 0 and 2π ($2/9\pi, 4/9\pi, 6/9\pi, 8/9\pi, 10/9\pi, 14/9\pi, 2\pi$). Each simulation was populated with a density of 70 animals km^{-2} , calculated from the equation in Damuth (1981) as the expected density of mammals of weighing 1 g. This density therefore represents a reasonable estimate of density of individuals, given that the smallest mammal is around 2 g (Jones *et al.*, 2009). A total of 3937 individuals per simulation were created which were placed randomly at the start of the simulation. Individuals were assigned 11 signal widths α between 0 and π ($1/11\pi, 2/11\pi, 3/11\pi, 4/11\pi, 5/11\pi, 6/11\pi, 7/11\pi, 8/11\pi, 9/11\pi, 10/11\pi, \pi$).

Each simulation lasted for N steps (14400) of duration T (15 minutes) giving a total duration of 150 days. The individuals moved within each step with a distance d , with an average speed, v . d , was sampled from a normal distribution with mean distance, $\mu_d = vT$, and standard deviation $\sigma_d = vT/10$. An average speed, $v = 40 \text{ km day}^{-1}$, was chosen as this is the largest day range of terrestrial animals (Carbone *et al.*, 2005), and represents the upper limit of realistic speeds. At the end step, individuals were allowed to either remain stationary for a time step (with a given probability, S), or change direction (in a uniform distribution with a maximum angle, A) between 0 and π . This resulted in 7 different movement models where: (1) simple movement, where S and $A = 0$; (2) stop-start movement, where (i) $S = 0.25, A = 0$, (ii) $S = 0.5, A = 0$, (iii) $S = 0.75, A = 0$; (3) random walk movement, where (i) $S = 0, A = \pi/3$, (ii) $S = 0, A = 2\pi/3$, (iii) $S = 0, A = \pi$. Individuals were counted as they moved in and out of the detection zone of the sensor per simulation.

We calculated the estimated animal density from the gREM by summing the number of captures per simulation and inputting these values into the correct gREM submodel. gREM accuracy was determined by comparing the density in the simulation with the estimated density. High accuracy is indicated by the mean difference between the estimated and actual values not being significantly different from zero (Wilcoxon signed-rank test). gREM precision was determined by the standard deviation of estimated densities. We used this method to compare the accuracy and precision of all the gREM submodels. As these submodels are derived for different combinations of α and θ , the accuracy and precision of the submodels was used to determine the impact of different values of α and θ .

The influence of the number of captures and animal movement models on accuracy and precision was investigated using 4 different gREM submodels representative of the range α and θ values (submodels NW1, SW1, NE1, and SE3, Figure 2). Using these four submodels, we calculated how long the simulation needed to run to generate a range of different capture numbers (from 10 to 100 captures in 10 unit intervals), and estimated animal density. These estimated densities were compared to the real density to assess the impact on the accuracy and precision of the gREM. The gREM assumes that individuals move continuously with straight-line movement (simple movement model) and we therefore assessed the impact of breaking the gREM assumptions. We used the four submodels to compare the accuracy and precision of a simple movement model, stop-start movement models and random walk movement models.

RESULTS

Analytical model. The equation for \bar{p} has been newly derived for each submodel in the gREM, except for the gas model and REM which have been calculated previously. However, many models, although derived separately, have the same expression for \bar{p} . Figure 4 shows the expression for \bar{p} in each case. The general equation for density, using the correct expression for \bar{p} is then substituted into eqn 3. Although more thorough checks are performed in Appendix S3, it can be seen that all adjacent expressions in Figure 4 are equal when expressions for the boundaries between them are substituted in.

279 **Simulation model.**

280 *gREM submodels.* All gREM submodels showed a high accuracy, i.e., the mean dif-
 281 ference between the estimated and actual values was not significantly different
 282 from zero across all models, corrected for multiple tests (all gREM sub models
 283 Wilcoxon signed-rank test, $p > 0.002$)(Figure 5). However, the precision of the sub-
 284 models do vary, where the gas model is the most precise and the SW7 sub model
 285 the least precise, having the smallest and the largest interquartile range, respec-
 286 tively (Figure 5). The standard deviation of the error between the estimated and
 287 true densities is strongly related to both the sensor and signal widths (Figure 6),
 288 such that larger widths have lower standard deviations (greater precision).

289 *Number of captures.* Within the four gREM submodels tested (NW1, SW1, SE3,
 290 NE1), the accuracy was not affected by the number of captures, where the mean
 291 difference between the estimated and actual values was not significantly differ-
 292 ent from zero across all capture rates, corrected for multiple tests (all gREM sub
 293 models Wilcoxon signed-rank test, $p > 0.008$)(Figure 7). However, the precision
 294 was dependent on the number of captures across all four of the gREM submod-
 295 els, where precision increases as number of captures increases (Figure 7). For all
 296 gREM submodels, the the coefficient of variation falls to 10% at 100 captures.

297 *Movement models.* Within the four gREM submodels tested (NW1, SW1, SE3, NE1),
 298 neither the accuracy or precision was affected by the amount of time spent sta-
 299 tionary. The mean difference between the estimated and actual values was not
 300 significantly different from zero for each category of stationary time (0, 0.25, 0.5
 301 and 0.75), corrected for multiple tests (all gREM sub models Wilcoxon signed-rank
 302 test, $p > 0.12$)(Figure 8a). Altering the maximum change in direction in each step
 303 (0, $\pi/3$, $2\pi/3$, and π) did not affect the accuracy or precision of the four gREM
 304 submodels tested (all gREM sub models Wilcoxon signed-rank test, $p > 0.05$)(Fig-
 305 ure 8b).

306 DISCUSSION

307 We have developed the gREM such that it can be used to estimate density from
 308 acoustic sensors and camera traps. This has entailed a generalisation of the gas

model and the REM in Rowcliffe *et al.* (2008) to be applicable to any combination of sensor width and signal directionality. We have used simulations to show, as a proof of principle, that these models are accurate and precise. The precision of the gREM was found to be dependent on the width of the sensor and the call, and the number of captures.

Analytical model. The gREM was derived for different combinations of α and θ resulting in 25 different submodels, the expression for \bar{p} are equal for many of these submodels resulting in eight different equations including the previously derived gas model and REM. These submodels were tested for consistency with adjacent expressions being equal at their boundaries. These new submodels will allow researchers to evaluate the absolute density of animals that have previously been difficult to study, such as bats (Clement & Castleberry, 2013), with noninvasive methods such as remote sensors. The gREM allows the data from acoustic detectors to be used where an animal has a directional calls, this could be used for a range of animals including songbirds (Blumstein *et al.*, 2011), and dolphins (Lammers & Au, 2003).

There are a number of possible extensions to the gREM which could be developed in the future. The original gas model was formulated for the case where both subjects, either animal and detector, or animal and animal, are moving (Hutchinson & Waser, 2007). Indeed any of the models with animals that are equally detectable in all directions ($\alpha = 2\pi$) can be trivially expanded for moving by substituting the sum of the average animal velocity and the sensor velocity for v as used here. However, when the animal has a directional call, as seen in both terrestrial and aquatic environments (Lammers & Au, 2003; Blumstein *et al.*, 2011), the extension becomes less simple. The approach would be to calculate again the mean profile width. However, for each angle of approach, one would have to average the profile width for an animal facing in any direction (i.e. not necessarily moving towards the sensor) weighted by the relative velocity of that direction. There are a number of situations where a moving detector and animal could occur, e.g. an acoustic detector towed from a boat when studying porpoises (Kimura *et al.*, 2014) or surveying bats from a moving car (Ahlen & Baagøe, 1999; ?).

340 An interesting but unstudied problem is edge effects caused by trigger delays
 341 (the delay between sensing an animal and attempting to record the encounter)
 342 (Rovero *et al.*, 2013) and time expansion acoustic detectors which repeatedly turn
 343 on an off during sampling (Ahlen & Baagøe, 1999). Both of these have potential
 344 biases as animals can move through the detection zone without being detected.
 345 The models herein are formulated assuming constant surveillance and so the error
 346 created by switching the sensor on and off quickly becomes negligible if the sensor
 347 is on for extended periods of time. For example, if it takes longer for the recording
 348 device to be switched on than the length of some animal calls there could be a
 349 systematic underestimation of density.

350 **Accuracy and Precision.** Based on our simulations we believe that the gREM has
 351 the potential to produce accurate estimates for many different species, using ei-
 352 ther camera traps or acoustic detectors. However the precision of the gREM dif-
 353 fered between submodels. For example, when the sensor and signal width were
 354 smaller than the precision of the model was reduced, so when choosing a sensor
 355 for use in a gREM study the detection width should be maximised, and if the study
 356 species has a narrow signal directionality other aspects of the study protocol, such
 357 as length of the survey, should be used to compensate.

358 The precision of the gREM is greatly affected by the number of captures that are
 359 collected, the coefficient of variation falls dramatically between 10 and 60 captures
 360 and then after this continues to slowly reduce. At 100 captures the submodels
 361 reach 10% coefficient of variation, considered to a very good level of precision
 362 (Thomas & Marques, 2012). Many current studies do not reach this level of pre-
 363 cision, with most studies reporting coefficient of variations greater than the 10%
 364 level (O'Brien *et al.*, 2003; Proctor *et al.*, 2010; Foster & Harmsen, 2012). The length
 365 of surveys in the field will need to be adjusted so that enough data can be collected
 366 to reach this level of precision. Populations of fast moving animals or populations
 367 with large densities will require less survey effort than those with slow moving or
 368 low densities.

369 The gREM was both accurate and precise for all the movement models we
 370 tested (stop-start movement and correlated random walks). However these move-
 371 ment models are still simple representations of true animal movement which are
 372 dependent on multiple factors such as behavioural state and and existence of
 373 home ranges (Smouse *et al.*, 2010). The accuracy of the gREM may be affected
 374 by the interaction between the movement model and the size of the detection ra-
 375 dius. We have studied a relatively long step length compared to the size of the
 376 detection radius, and therefore the chance of catching the same animal multiple
 377 times within a short space of time was reduced and there is little affect on the pre-
 378 cision of the model (Figure 8b). However if the ratio of step length to detection
 379 radius was smaller then this may decrease the precision of the model, however
 380 this should not decrease its accuracy.

381 Although we have used simulations to validate the gREM submodels, much
 382 more robust testing is needed. Although difficult, proper field test validation
 383 would be required before the models could be fully trusted. The REM (Rowcliffe
 384 *et al.*, 2008) has already been field tested, and both Rowcliffe *et al.* (2008) and Zero
 385 *et al.* (2013) both found that the REM was an effective manner of estimating ani-
 386 mal densities (Rowcliffe *et al.*, 2008; Zero *et al.*, 2013). In some taxa gold standard
 387 methods of estimating animal density exist, such as capture mark recapture (Soll-
 388 mann *et al.*, 2013). Where these gold standard exist or true numbers are known,
 389 a simultaneous gREM study could be completed to test the accuracy under field
 390 conditions, similar to the tests that Rowcliffe *et al.* (2008) completed with the REM.
 391 An easier way to continue to evaluate the models is to run more extensive simula-
 392 tions which break the assumptions of the analytical models. The main element that
 393 cannot be analytically treated is the complex movement of real animals. There-
 394 fore testing these methods against true animal traces, or more complex movement
 395 models would be required.

396 Within the simulation we have assumed an equal density across the entire world,
 397 however in a field environment the situation would be much more complex, with
 398 additional variation coming from local changes in density between camera sites.
 399 We allowed the sensor to be stationary and on all the time, negating the trigger-
 400 ing, and time expansion issues that could exist in real life. In the simulation we

ran the speed of the animal as 40 km day^{-1} , the largest day range of terrestrial animals (Carbone *et al.*, 2005). Other speed values should not alter the accuracy of the gREM (precision would be affected, all else being equal, since slower speeds produce fewer records). We also assume perfect knowledge of the average speed of an animal and size of the detection zone, and instant triggering of the camera. All of which may lead to possible bias or a decrease in precision.

Implications for conservation. The gREM is available for the estimation of density of a number of taxa where no, or few, accurate methods currently exist to measure absolute animal density (Thomas & Marques, 2012). The species that can now be studied may be of importance to conservation, for example current methods of density estimation for the threatened Franciscana dolphin may result in underestimation of numbers (Crespo *et al.*, 2010). This new method may be important for the study of zoonotic diseases, for example estimating population sizes of bats, which are important reservoir of infectious disease that affect humans, livestock and wildlife (Calisher *et al.*, 2006). In addition, the gREM will make it possible to measure the density of animals which may be useful in quantifying ecosystem services, such as studying the levels of songbirds which are known to have a positive influence on pest control in coffee production (Jirinec *et al.*, 2011). The gREM is suitable for any species that would be consistently recorded within range of a detector, such as bats (Kunz *et al.*, 2009), songbirds (Buckland & Handel, 2006), whales (Marques *et al.*, 2009) or forest primates (Hassel-Finnegan *et al.*, 2008). With increasing technological capabilities, this list of species is likely to increase dramatically.

Importantly the camera trapping and acoustic recording that the gREM use are noninvasive and do not require individual marking (Jewell, 2013) or naturally identifying marks (as required for mark-recapture models). This makes them suitable for large, continuous monitoring projects with limited human resources (Kelly *et al.*, 2012). It also makes them suitable for species that are under pressure, species that cannot naturally be individually recognised or species that are difficult or dangerous to catch (Thomas & Marques, 2012).

1. ACKNOWLEDGMENTS

REFERENCES

- Acevedo, M.A. & Villanueva-Rivera, L.J. (2006) Using automated digital recording systems as effective tools for the monitoring of birds and amphibians. *Wildlife Society Bulletin*, **34**, 211–214.
- Ahlen, I. & Baagøe, H.J. (1999) Use of ultrasound detectors for bat studies in europe: experiences from field identification, surveys, and monitoring. *Acta Chiropterologica*, **1**, 137–150.
- Anderson, D.R. (2001) The need to get the basics right in wildlife field studies. *Wildlife Society Bulletin*, pp. 1294–1297.
- Barlow, J. & Taylor, B. (2005) Estimates of sperm whale abundance in the north-eastern temperate pacific from a combined acoustic and visual survey. *Marine Mammal Science*, **21**, 429–445.
- Blumstein, D.T., Mennill, D.J., Clemens, P., Girod, L., Yao, K., Patricelli, G., Deppe, J.L., Krakauer, A.H., Clark, C., Cortopassi, K.A. *et al.* (2011) Acoustic monitoring in terrestrial environments using microphone arrays: applications, technological considerations and prospectus. *Journal of Applied Ecology*, **48**, 758–767.
- Brusa, A. & Bunker, D.E. (2014) Increasing the precision of canopy closure estimates from hemispherical photography: Blue channel analysis and under-exposure. *Agricultural and Forest Meteorology*, **195**, 102–107.
- Buckland, S.T. & Handel, C. (2006) Point-transect surveys for songbirds: robust methodologies. *The Auk*, **123**, 345–357.
- Buckland, S.T., Marsden, S.J. & Green, R.E. (2008) Estimating bird abundance: making methods work. *Bird Conservation International*, **18**, S91–S108.
- Calisher, C., Childs, J., Field, H., Holmes, K. & Schountz, T. (2006) Bats: important reservoir hosts of emerging viruses. *Clinical microbiology reviews*, **19**, 531–545.
- Carbone, C., Cowlshaw, G., Isaac, N.J. & Rowcliffe, J.M. (2005) How far do animals go? Determinants of day range in mammals. *The American Naturalist*, **165**, 290–297.
- Clark, C.W. (1995) Application of US Navy underwater hydrophone arrays for scientific research on whales. *Reports of the International Whaling Commission*, **45**,

- 210–212.
- Clement, M.J. & Castleberry, S.B. (2013) Estimating density of a forest-dwelling bat: a predictive model for rafinesque’s big-eared bat. *Population Ecology*, **55**, 205–215.
- Crespo, E.A., Pedraza, S.N., Grandi, M.F., Dans, S.L. & Garaffo, G.V. (2010) Abundance and distribution of endangered franciscana dolphins in argentine waters and conservation implications. *Marine Mammal Science*, **26**, 17–35.
- Cutler, T.L. & Swann, D.E. (1999) Using remote photography in wildlife ecology: a review. *Wildlife Society Bulletin*, pp. 571–581.
- Damuth, J. (1981) Population density and body size in mammals. *Nature*, **290**, 699–700.
- Depraetere, M., Pavoine, S., Jiguet, F., Gasc, A., Duvail, S. & Sueur, J. (2012) Monitoring animal diversity using acoustic indices: implementation in a temperate woodland. *Ecological Indicators*, **13**, 46–54.
- Elphick, C.S. (2008) How you count counts: the importance of methods research in applied ecology. *Journal of Applied Ecology*, **45**, 1313–1320.
- Everatt, K.T., Andresen, L. & Somers, M.J. (2014) Trophic scaling and occupancy analysis reveals a lion population limited by top-down anthropogenic pressure in the limpopo national park, mozambique. *PloS one*, **9**, e99389.
- Foster, R.J. & Harmsen, B.J. (2012) A critique of density estimation from camera-trap data. *The Journal of Wildlife Management*, **76**, 224–236.
- Harris, D., Matias, L., Thomas, L., Harwood, J. & Geissler, W.H. (2013) Applying distance sampling to fin whale calls recorded by single seismic instruments in the northeast atlantic. *The Journal of the Acoustical Society of America*, **134**, 3522–3535.
- Hassel-Finnegan, H.M., Borries, C., Larney, E., Umponjan, M. & Koenig, A. (2008) How reliable are density estimates for diurnal primates? *International Journal of Primatology*, **29**, 1175–1187.
- Hutchinson, J.M.C. & Waser, P.M. (2007) Use, misuse and extensions of “ideal gas” models of animal encounter. *Biological Reviews of the Cambridge Philosophical Society*, **82**, 335–359.

- 493 Jewell, Z. (2013) Effect of monitoring technique on quality of conservation science.
494 *Conservation Biology*, **27**, 501–508.
- 495 Jirinec, V., Campos, B.R. & Johnson, M.D. (2011) Roosting behaviour of a migratory
496 songbird on jamaican coffee farms: landscape composition may affect delivery
497 of an ecosystem service. *Bird Conservation International*, **21**, 353–361.
- 498 Jones, K.E., Bielby, J., Cardillo, M., Fritz, S.A., O'Dell, J., Orme, C.D.L., Safi, K.,
499 Sechrest, W., Boakes, E.H., Carbone, C. *et al.* (2009) PanTHERIA: a species-level
500 database of life history, ecology, and geography of extant and recently extinct
501 mammals: Ecological archives e090-184. *Ecology*, **90**, 2648–2648.
- 502 Karanth, K. (1995) Estimating tiger (*Panthera tigris*) populations from camera-trap
503 data using capture–recapture models. *Biological Conservation*, **71**, 333–338.
- 504 Kelly, M.J., Betsch, J., Wultsch, C., Mesa, B. & Mills, L.S. (2012) Noninvasive sam-
505 pling for carnivores. *Carnivore ecology and conservation: a handbook of techniques*
506 (*L Boitani and RA Powell, eds*) Oxford University Press, New York, pp. 47–69.
- 507 Kessel, S., Cooke, S., Heupel, M., Hussey, N., Simpfendorfer, C., Vagle, S. & Fisk, A.
508 (2014) A review of detection range testing in aquatic passive acoustic telemetry
509 studies. *Reviews in Fish Biology and Fisheries*, **24**, 199–218.
- 510 Kimura, S., Akamatsu, T., Dong, L., Wang, K., Wang, D., Shibata, Y. & Arai, N.
511 (2014) Acoustic capture-recapture method for towed acoustic surveys of echolo-
512 cating porpoises. *The Journal of the Acoustical Society of America*, **135**, 3364–3370.
- 513 Kunz, T.H., Betke, M., Hristov, N.I. & Vonhof, M. (2009) Methods for assessing
514 colony size, population size, and relative abundance of bats. *Ecological and be-*
515 *havioral methods for the study of bats* (*TH Kunz and S Parsons, eds*) 2nd ed Johns
516 Hopkins University Press, Baltimore, Maryland, pp. 133–157.
- 517 Lammers, M.O. & Au, W.W. (2003) Directionality in the whistles of hawaiian spin-
518 ner dolphins (*stenella longirostris*): A signal feature to cue direction of move-
519 ment? *Marine Mammal Science*, **19**, 249–264.
- 520 Lewis, T., Gillespie, D., Lacey, C., Matthews, J., Danbolt, M., Leaper, R.,
521 McLanaghan, R. & Moscrop, A. (2007) Sperm whale abundance estimates from
522 acoustic surveys of the ionian sea and straits of sicily in 2003. *Journal of the Ma-*
523 *rine Biological Association of the United Kingdom*, **87**, 353–357.

- Manzo, E., Bartolommei, P., Rowcliffe, J.M. & Cozzolino, R. (2012) Estimation of population density of european pine marten in central italy using camera trapping. *Acta Theriologica*, **57**, 165–172.
- Marcoux, M., Auger-Méthé, M., Chmelnitsky, E.G., Ferguson, S.H. & Humphries, M.M. (2011) Local passive acoustic monitoring of narwhal presence in the canadian arctic: a pilot project. *Arctic*, pp. 307–316.
- Marques, T.A., Munger, L., Thomas, L., Wiggins, S. & Hildebrand, J.A. (2011) Estimating North Pacific right whale (*Eubalaena japonica*) density using passive acoustic cue counting. *Endangered Species Research*, **13**, 163–172.
- Marques, T.A., Thomas, L., Ward, J., DiMarzio, N. & Tyack, P.L. (2009) Estimating cetacean population density using fixed passive acoustic sensors: An example with Blainville’s beaked whales. *The Journal of the Acoustical Society of America*, **125**, 1982–1994.
- O’Brien, T.G., Kinnaird, M.F. & Wibisono, H.T. (2003) Crouching tigers, hidden prey: Sumatran tiger and prey populations in a tropical forest landscape. *Animal Conservation*, **6**, 131–139.
- O’Farrell, M.J. & Gannon, W.L. (1999) A comparison of acoustic versus capture techniques for the inventory of bats. *Journal of Mammalogy*, pp. 24–30.
- Proctor, M., McLellan, B., Boulanger, J., Apps, C., Stenhouse, G., Paetkau, D. & Mowat, G. (2010) Ecological investigations of grizzly bears in canada using dna from hair, 1995-2005: a review of methods and progress. *Ursus*, **21**, 169–188.
- Purvis, A., Gittleman, J.L., Cowlshaw, G. & Mace, G.M. (2000) Predicting extinction risk in declining species. *Proceedings of the Royal Society of London Series B: Biological Sciences*, **267**, 1947–1952.
- R Development Core Team (2010) *R: A Language And Environment For Statistical Computing*. R Foundation For Statistical Computing, Vienna, Austria. ISBN 3-900051-07-0.
- Richter-Dyn, N. & Goel, N.S. (1972) On the extinction of a colonizing species. *Theoretical Population Biology*, **3**, 406–433.
- Rogers, T.L., Ciaglia, M.B., Klinck, H. & Southwell, C. (2013) Density can be misleading for low-density species: benefits of passive acoustic monitoring. *Public Library of Science One*, **8**, e52542.

- 556 Rovero, F., Zimmermann, F., Berzi, D. & Meek, P. (2013) " which camera trap type
557 and how many do i need?" a review of camera features and study designs for a
558 range of wildlife research applications. *Hystrix*.
- 559 Rowcliffe, J.M. & Carbone, C. (2008) Surveys using camera traps: are we looking
560 to a brighter future? *Animal Conservation*, **11**, 185–186.
- 561 Rowcliffe, J., Field, J., Turvey, S. & Carbone, C. (2008) Estimating animal density
562 using camera traps without the need for individual recognition. *Journal of Ap-
563 plied Ecology*, **45**, 1228–1236.
- 564 Schmidt, B.R. (2003) Count data, detection probabilities, and the demography, dy-
565 namics, distribution, and decline of amphibians. *Comptes Rendus Biologies*, **326**,
566 119–124.
- 567 Smouse, P.E., Focardi, S., Moorcroft, P.R., Kie, J.G., Forester, J.D. & Morales, J.M.
568 (2010) Stochastic modelling of animal movement. *Philosophical Transactions of the
569 Royal Society B: Biological Sciences*, **365**, 2201–2211.
- 570 Soisalo, M.K. & Cavalcanti, S. (2006) Estimating the density of a jaguar population
571 in the Brazilian Pantanal using camera-traps and capture-recapture sampling in
572 combination with GPS radio-telemetry. *Biological Conservation*, **129**, 487–496.
- 573 Sollmann, R., Gardner, B., Chandler, R.B., Shindle, D.B., Onorato, D.P., Royle, J.A.
574 & O’Connell, A.F. (2013) Using multiple data sources provides density estimates
575 for endangered florida panther. *Journal of Applied Ecology*, **50**, 961–968.
- 576 SymPy Development Team (2014) *SymPy: Python library for symbolic mathematics*.
- 577 Thomas, L. & Marques, T.A. (2012) Passive acoustic monitoring for estimating an-
578 imal density. *Acoustics Today*, **8**, 35–44.
- 579 Trolle, M. & Kéry, M. (2003) Estimation of ocelot density in the Pantanal using
580 capture-recapture analysis of camera-trapping data. *Journal of mammalogy*, **84**,
581 607–614.
- 582 Trolle, M., Noss, A.J., Lima, E.D.S. & Dalponte, J.C. (2007) Camera-trap studies of
583 maned wolf density in the Cerrado and the Pantanal of Brazil. *Biodiversity and
584 Conservation*, **16**, 1197–1204.
- 585 Walters, C.L., Collen, A., Lucas, T.C.D., Mroz, K., Sayer, C.A. & Jones, K.E. (2013)
586 Challenges of using bioacoustics to globally monitor bats. *Bat Evolution, Ecology,
587 and Conservation*, pp. 479–499. Springer.

- 588 Wright, S.J. & Hubbell, S.P. (1983) Stochastic extinction and reserve size: a focal
589 species approach. *Oikos*, pp. 466–476.
- 590 Yapp, W. (1956) The theory of line transects. *Bird study*, **3**, 93–104.
- 591 Zero, V.H., Sundaresan, S.R., O'Brien, T.G. & Kinnaird, M.F. (2013) Monitoring
592 an endangered savannah ungulate, Grevy's zebra (*Equus grevyi*): choosing a
593 method for estimating population densities. *Oryx*, **47**, 410–419.

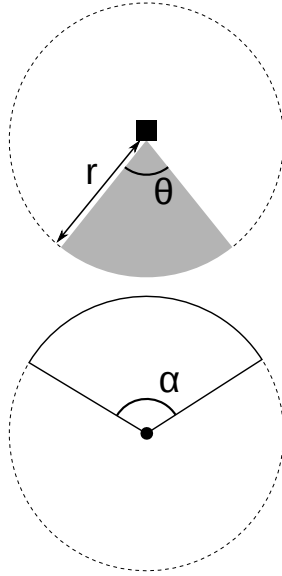


FIGURE 1. Representation of sensor detection width and animal signal width. The filled square and circle represent a sensor and an animal, respectively; θ , sensor detection width (radians); r , sensor detection distance; dark grey shaded area, sensor detection zone; α , animal signal width (radians). Dashed lines around the filled square and circle represents the maximum extent of θ and α , respectively.

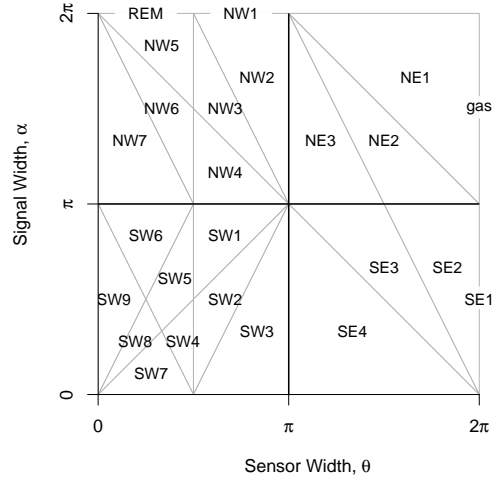


FIGURE 2. Locations where derivation of the average profile \bar{p} is the same for different combinations of sensor detection width and animal signal width. Symbols within each polygon refer to each gREM submodel named after their compass point, except for Gas and REM which highlight the position of these previously derived models within the gREM. Symbols on the edge of the plot are for submodels with $\alpha, \theta = 2\pi$

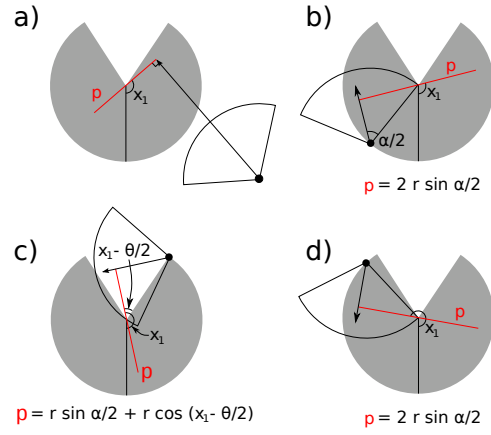


FIGURE 3. An overview of the derivation of SE2. The filled circles represent animals, with the animal signal shown as an unfilled sector and the direction of movement shown as an arrow. The detection zone of the sensor is shown as filled grey sectors with a detection distance of r . The vertical black line within the circle shows the direction the sensor is facing; θ , sensor detection width; α , animal signal width. The profile p (the line an animal must pass through in order to be captured) is shown in red and x_1 is the focal angle, where (a) shows the location of x_1 . The derivation of p changes as the animal approaches the sensor from different directions where (b) is the derivation of p when x_1 is in the interval $[\frac{\pi}{2}, \frac{\pi}{2} + \frac{\theta}{2} - \frac{\alpha}{2}]$, (c) p when x_1 is in the interval $[\frac{\pi}{2} + \frac{\theta}{2} - \frac{\alpha}{2}, \frac{5\pi}{2} - \frac{\theta}{2} - \frac{\alpha}{2}]$ and (d) p when x_1 is in the interval $[\frac{5\pi}{2} - \frac{\theta}{2} - \frac{\alpha}{2}, \frac{3\pi}{2}]$. The resultant equation for p is shown beneath each figure.

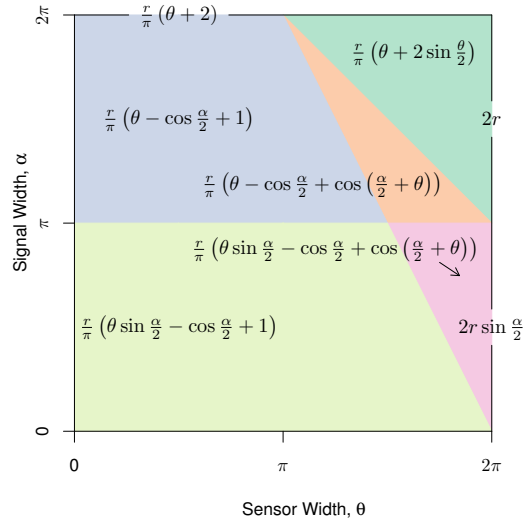


FIGURE 4. Expressions for the average profile width, \bar{p} , given sensor and signal widths. Despite independent derivation within each block, many models result in the same expression. These are collected together and presented as one block of colour. Expressions on the edge of the plot are for submodels with $\alpha, \theta = 2\pi$.

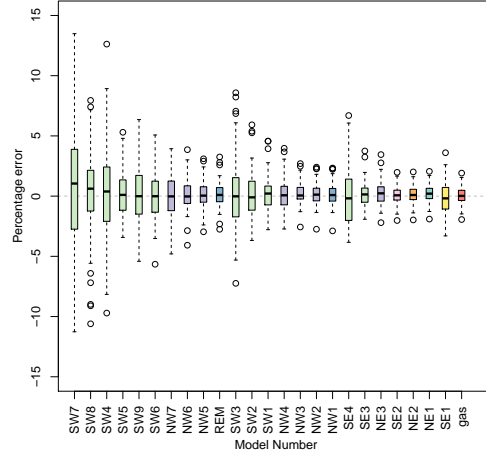


FIGURE 5. Simulation model results of the accuracy and precision for gREM submodels. The percentage error between estimated and true density for each gREM submodel is shown within each box plot, where the black line represents the median percentage error across all simulations, boxes represent the the middle 50% of the data, whiskers represent variability outside the upper and lower quartiles with outliers plotted as individual points. Box colours correspond to the expressions for average profile width \bar{p} given in Figure 4.

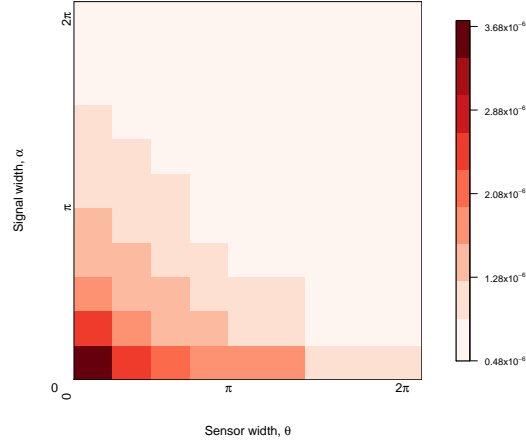


FIGURE 6. Simulation model results of the gREM precision given a range of sensor and signal widths, shown by the standard deviation of the error between the estimated and true densities. Standard deviations are shown from deep red to pink, representing high to low values between 0.483×10^{-6} to 3.74×10^{-6} .

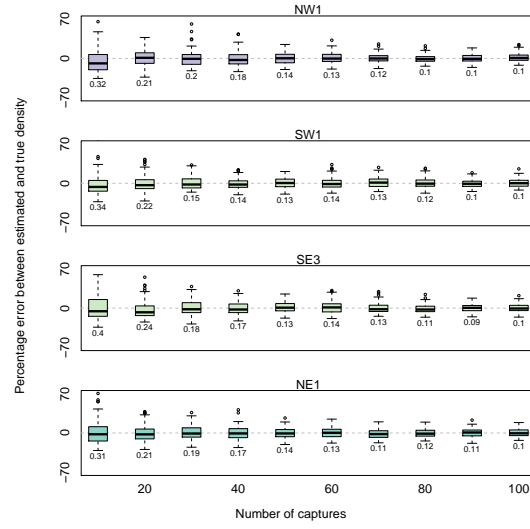


FIGURE 7. Simulation model results of the accuracy and precision of four gREM submodels (NW1, SW1, SE3 and NE1) given different numbers of captures. The percentage error between estimated and true density within each gREM sub model for capture rate is shown within each box plot. Sensor and signal widths vary between submodels. The number beneath each plot represents the coefficient of variation. The colour of each box plot corresponds to the expressions for average profile width \bar{p} given in Figure 4.

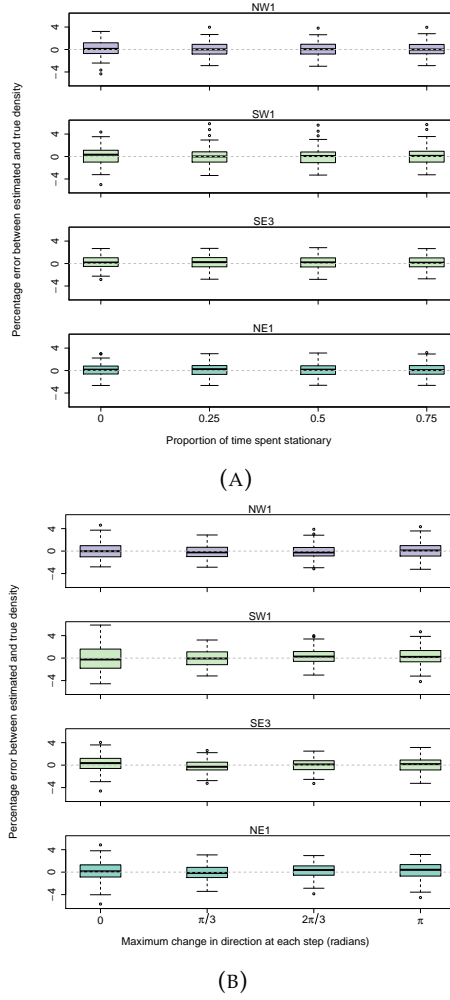


FIGURE 8. Simulation model results of the accuracy and precision of four gREM submodels (NW1, SW1, SE3 and NE1) given different movement models where (A) amount of time spent stationary (stop-start movement) and (B) maximum change in direction at each step (correlated random walk model). The percentage error between estimated and true density within each gREM sub model for the different movement models is shown within each box plot. The simple model is represented where time and maximum change in direction equals 0. The colour of each box plot corresponds to the expressions for average profile width \bar{p} given in Figure 4.